Fracture toughness K_{IC} of cemented carbide WC-Co

S. Doi & M. Yasuoka
Oita University, Japan
and Fujikoshi Co., Japan

Abstract

Rotating bending fatigue test was carried out using the cemented carbide WC-Co in ultra-long life. A carbide metal WC has many defects on the boundary. A crack initiates from these defects, and propagates belong the boundary. Fatigue limit does not exist. The boundary slips easily, and is weak to sharing force. The fatigue crack propagation rate (da/dN) cannot calculate. But, fracture toughness K_{IC} can calculate from relationship fractal dimension or Hurst number (localized wavelets transformation) and yield area. Yield area of fracture in ultralong Nf=2.05×107 broad Origin of fracture is surface defects. When $K_{IC}>K_{max}$ in surface stands up, the crack in the plane stress propagate. The fatigue strength of WC cemented carbide is obeyed to weakest link model of defects. Because, even if it supposes that it was worked the cyclic stress over the fatigue strength, the fatigue fracture did not always happen. If K_{max}/K_{IC}=const. stands up, a small crack is equivalent to a small defect, and fracture of material is induced by initiated crack. By the fractal dimension analysis, the phenomenon of fracture mechanisms will be clear.
Keywords: fracture toughness, cemented carbide WC, double bending S-N curve, fractal dimension, Hurst number.

1 Introduction

Cemented carbide occupies an important position as an element of tool, but is not studied as much as high-hardness, high-toughness carbon steel. As regards the method for evaluating cemented carbide, either transverse fracture strength or fracture toughness by impact value is used. In either case, Palmqvist [1], method which consists of measuring the length of cracks produced at the corner of a

WIT Transactions on Engineering Sciences, Vol 64, © 2009 WIT Press
www.witpress.com, ISSN 1743-3533 (on-line)
doi:10.2495/MC090211

Vickers impression, is used. There are also a variety of other techniques for introducing initial cracks, and each of them has its advantages and disadvantages. According to Chermant et al [2], who studied variations of fracture toughness K_{IC} ,due to differences in particle size of WC-Co material which was used in the present study, the larger the particle size of WC the greater K_{IC}, even with the same Co%. One reason for it is the suspected presence of something other than iron-based metals is because the grain boundary binding energy increases. However, the notion of weakest link model is generally accepted against unstable fracture of materials such as ceramics, etc., because most of the factors are represented by intergranular fractures due to second-phase granular action by segregation of Co. As described above, the method of determination of fracture toughness is similar that used in quasi-static tests, and fracture toughness is calculated and defined by the length of the crack. However, because the fracture toughness value variable in depending on whether the point of origin of the crack is on the surface or inside the material, those factors should be determined from the conditions of fatigue fracture mechanisms, its fracture mechanisms was clarified by the small-scale yield area to large-scale yield area based on a fractal dimension analysis as a method of fractography. The boundary determination of the plastic zone was made by noting changes in fractal dimension with reference to the image by using a confocal laser microscope. The method using photographs cannot be said to be an accurate method because it involves a change of dimension, but it enables researchers to pass judgment on whether an unstable fracture has been produced based on whether a position deviated from the linear relation or not.

2 Test specimen and fatigue test

As a test specimen, we used bending fatigue test pieces of smooth rotation finished in the shape and dimension with a parallel portion of 5 mm indicated in Figure. 1.

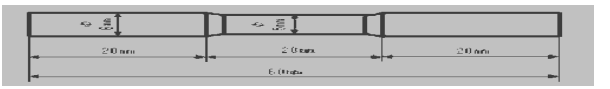

Figure 1: Rotating bending fatigue test piece.

Figure 2 shows a micrographic photo observed at a magnification of 1500 of the test piece cut out in the axial direction after the test and etched with Murakami's reagent.

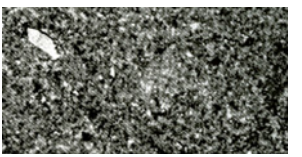

Figure 2: Micrograph of test piece [×1500].

The white insoluble particles are believed to be residues of Cr. They remain as so-called second-phase particles.

Table 1: Chemical Components of carbided carbon WC.

WC	VC	Cr_3C_2 %	Co %
87.5	0.7	0.8	11

Table 2: Mechanical properties.

Applications	Vickers hardness	Transvers rupture strength	Density	Fracture toughness	Coefficient of thermal expansion	Coefficient of heat conductivity	Young's modulus
		GPa		$MPam^{1/2}$	$\times 10^{-6}/K$	W/mk	GPa
Various quality	1690–1725 / 1708	3.1	14	9.5	5.6	63	550

A lot of pores with fine particles are observed generally. The results of the fracture toughness test by Chermant et al. [2] mentioned earlier agree with the results obtained in the present study.

$$K_{IC} = \phi \ \sigma \sqrt{a} \tag{1}$$

In that example, calculated values of a+Δa obtained by changing the amount of load in the measured values of Vickers hardness are plotted. The axis(x,y) in Figure 3 is arbitrary. From those values, the value of fracture toughness comes to 9 $MPam^{1/2}$ in the case where the particle size of WC is 1 μm. Moreover, mention made of a study used for estimating the maximum strength from the relation with the transverse rupture strength by putting the pores as a defective surface area of $A^{-1/4}(\mu m^{-1/2})$. This study is subject to the condition that not only the fracture toughness but also the transverse rupture strength are large. In any case, the test method described above is quasistatic, and is not intended for fatigue strength. In the present study, we propose a method for determining the dimensions of plastic zone on the basis of the information which appeared in the fractured face as a result of fatigue test. The value of fracture toughness can be determined from them.

3 Test results and discussion

3.1 Ultra-long of S-N curve

Fig. 3 shows an S-N curve. Two test pieces fractured as a result of fatigue test by rotating bending were prepared by changing the stress level. For the horizontal part, Murakami proposed a method which consists of giving a critical value of progress of crack from the regression.

Statistics of extremes is used in order to provide an estimated value of fatigue test piece from surface area of the pore. This method is currently accepted as $\sqrt{}$area method [2]. As a result of calculations made by using the fatigue limit

evaluation formula in the case of the presence of some interposed material, an S-N curve as shown in Figure. 3, in general the shape of a two-stage bent type was obtained. However this cannot be considered as a detailed test result, partly because there is no reason to believe that any stoppage of crack takes place, judging from the fact that a fracture is produced immediately if some crack is initiated. By comparing with the mentioned above test results of other high-hardness , high-strength materials, that reason may be acceptable. However, based on reports of an example in which the material is bent in double stages as SNCM heat-treated material, among various raw materials, it is presumed that the pattern in the shape of stripe observed on the present test specimen shows a trace of progress and propagation of a crack. By the left in Figure 4, we can see that the face with propagation of crack stands on a different level.

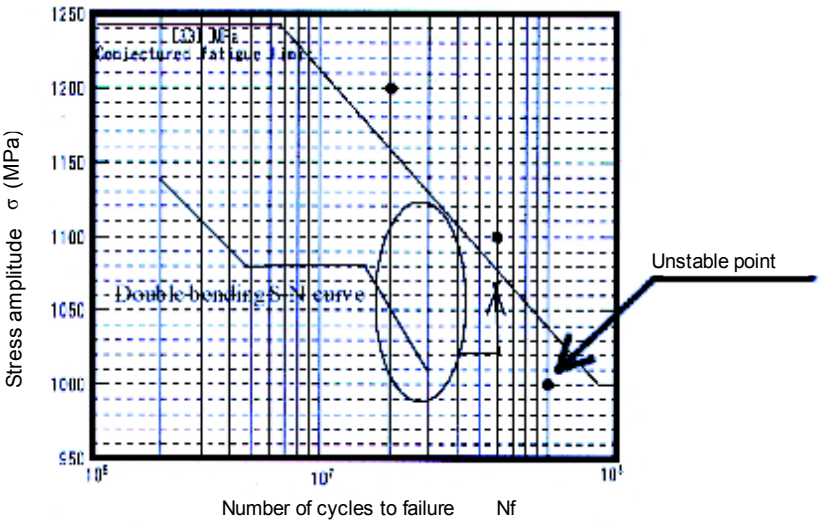

Figure 3: S-N curve in ultra-long Nf.

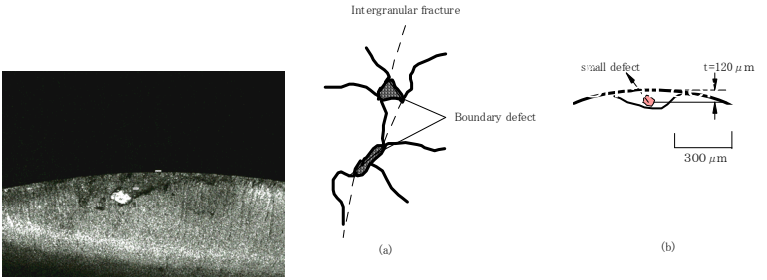

(a) (b)

Figure 4: Internal defect of Co.

4 Fracture toughness K_{IC}

4.1 Calculation method of fracture toughness K_{IC}

Description will be made of a method for estimating the fracture toughness value by fractography. A crack propagation pattern is left on the fracture by fatigue. If that information can be obtained quantitatively, it would be useful as a reliability evaluation method. It is often the case that, regarding propagation of cracks, the material characteristics are described from a da/dN-ΔK_{IC} diagram by checking the propagation rate of cracks on the surface of the specimen. In any case, a method which consists of describing the material characteristics by formulation lacks in description having unified universality. For that reason, we aimed at calculating the fracture toughness value showing the material characteristics by the method of image diagnosis and numerical expression, and studying it as fatigue fracture toughness value. Because fatigue fractures continuously change from small-scale yielding to large-scale yielding and their traces are left on the fracture, this is one of the reasons for adopting them as information. In this regard, a scanning confocal laser microscope is extremely effective. That is because it enables to easily visualize the height information which is one of the characteristics of the confocal type. If time-differential pictures are available, even approximation of the propagation rate of cracks may become possible, but this study does not go that for. A distribution spread of the yield area can be obtained in the form of a picture. Therefore, we applied and performed a method of numerical image analysis regarding finding of the magnitude of yield area. In the micrographic in Figure 4, there is a difference in brightness which seems to indicate formation of a plastic zone. The expanded schematic diagram (B) of the plastic zone away from the starting point shows an example of cracking in shell pattern with formation of intercrystalline cracks. At the central part of the defect, a fine white starting point is found and a black portion of the plastic zone is observed. Its dimension is approximately 25 μm and generally agrees with the results of fractal dimension. Furthermore, in the brittle fracture picture (A) at a position distant from the starting point, black patterns in stripes similar to crazing patterns can be observed. Those black patterns in stripes show spreading in a direction perpendicular to the direction of propagation of cracks, but they are different from ductile fracture type striation. This type of cemented carbide material is quite brittle against shearing, and it is rather difficult to visually find the dimensions of a fine yield area. In the present study, no fine yield area can be observed from Fig. 3, but this is believed to be something counted in the category of fatigue. There is no area showing generation, agglomeration, and propagation of cracks, and it is presumed that an unstable fracture takes place simultaneously as a result of intergranular cracks. In addition, as shown in the schematic diagram in Figure. 4(B), a fine crack (abnormality of Co) of insoluble metal compound, indicated in Figure. 4(A), which existed at a position approximately 120 μm from the surface in the case of cyclic stress of σs = 1100 MPa, was observed. Therefore the method of calculation of surface area of the defect as well as of the fracture toughness value will be described briefly. It

consists of checking the relationship between the fractal dimension and the dimension of fine yield area by grid-square analysis by transforming a 3-dimensional image of the scanning confocal laser microscope into peak-to-peak.

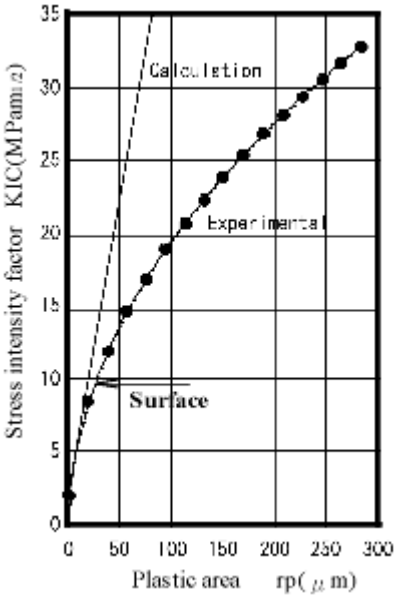

Figure 5: Relationship fracture toughness K_{IC} and plastic zone r_p (internal origin).

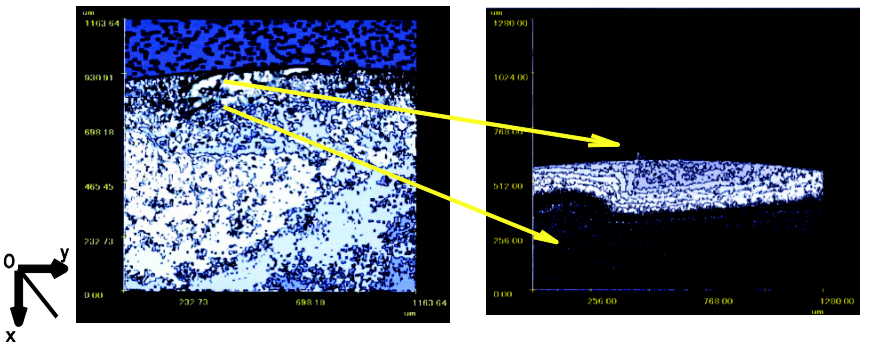

Figure 6: Photograph of surface origin [σ_s=1100 MPa].

height information, and calculating the fracture toughness value by the following formula:

$$w_p = \frac{\pi}{8}\left(\frac{K_{IC}}{\sqrt{3}\,\sigma_Y}\right)^2 \qquad (2)$$

where, formula (2) is an effective formula, σ_y is an effective value, and r_p is a half length of fine yield area.. In addition, as maximum allowable stress:

$$K_{max}=F\,\sigma_0\sqrt{\pi a} \tag{3}$$

where, F is a correction coefficient, set for $a<w_p$

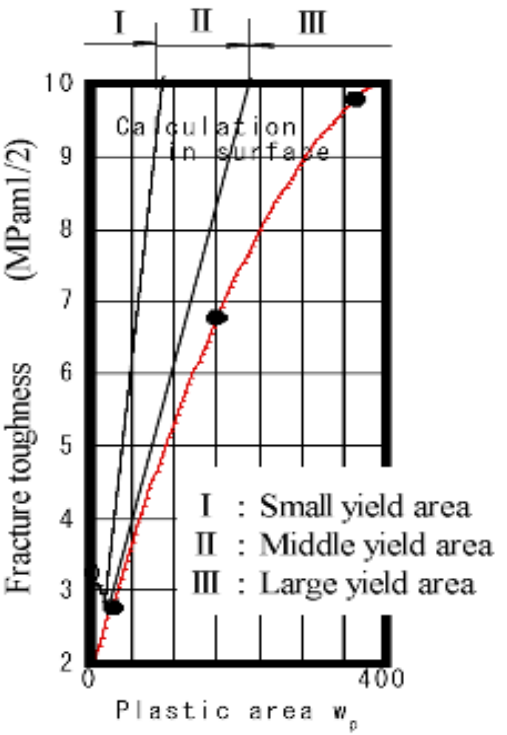

Figure 7: Relationship fracture toughness and plastic zone w_p(surface origin).

If $K_{IC} > K_{max}$ is established, it is defined as non fracturing stress. At that time, dimension of the defect is given as one, K_{max} it becomes a very small value. If you define the fine yield area as $Wp=x_a+r_p$ from the Dugdale model, the calculation is made by using $a+r_p$, on the condition of $r_p>>a$. In the case of $K_{IC} = K_{max}$, it shows that the crack does not propagate beyond this area. Namely, formula (4) gives conditions of unstable fracture. By calculating K_{max} / K_{IC} from the relation of Figure. 5, one obtains a = 1.1215 which satisfies the conditions. The spreading of the yield area is not clear from Fig. 6(a), but a pattern in stripe due to a difference of height appears.

The distribution of spreading can be understood if the image is turned into a confocal image, however, it is impossible to read up to the dimension rp of

small-scale yielding. We therefore decided to determine the fractal dimension and a for it, to find the K_{IC} value. In that case, the fracture toughness value taken seems to be the value at r_p = 25 μm and approximately 3 $MPam^{1/2}$. In this way, a difference is produced in fracture toughness value between surface type and

$$s_0=1.390s_y \quad \ldots\ldots\ldots\ldots \quad (4)$$

internal type, and one of the reasons for it is that the fracture toughness value is determined by the surface stress and the state of surface strain. If the fracture toughness value is the same , the relation of K_{IC} (inter) = 1/9 K_{IC} (surf) is about established.

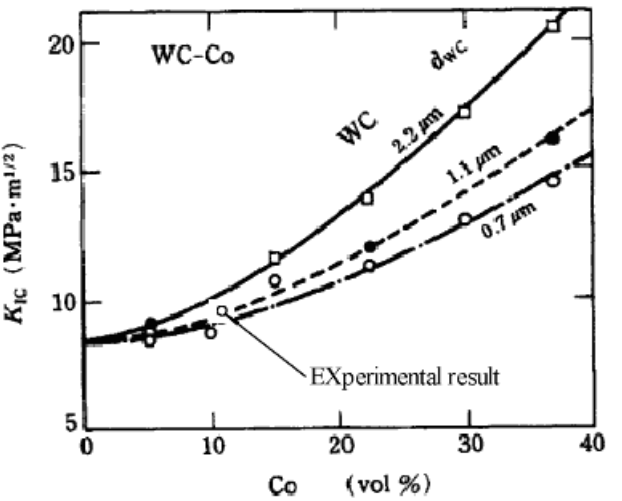

Figure 8: Typesetting author's value on Chermant et al. [2].

5 Observations

In the present study, we proposed a method of calculating the fracture toughness value from the yield area of a fracture by fractal dimension analysis. To check the characteristics of the fracture in more detail, it is necessary to expand the calculation up to the Hurst number. However, since the numerical values are smoothened to average the changes if the calculation is expanded up to the Hurst number, we deleted the noise on the way by moving the average in a way to show the peak-to-peak height. In this connection, we obtained 0.3 ($0<d_H<1$) as the Hurst number by calculation. If the Hurst number comes close to 1, it causes fluctuation and there is progress. From the stand point of analysis of numerical image, it becomes meaningless because the high information is smoothed. Therefore, we tried a method enabling us to make proper analysis without destroying the information characteristics of the fracture. Because the original information is that of roughness parameters we made by fetching surface roughness into the basic information, we obtained excellent Figures 5 and 7.

Those results were transplanted in Figure 8 of Chermant et al. The fracture toughness value calculated on the basis of the data obtained from the results of fatigue test turned out to be an excellent one, clearly showing that there is no need of performing any particular fracture mechanical experiment. However, ambiguity of fractal dimension analysis makes it necessary to calculate from a distribution chart in the direction q by fixing a coordinate centering on the starting point. Data processing was simplified by a method of collectively handling peak coordinates, which is used as one of the methods for omitting such troublesome steps. Although the fatigue limit estimation method of S-N curve described in paragraph 3.1 gives a description of approximately s_w=1330 MPa, from the scope of the present study, there is a report that, in reality, that figure comes to approximately 1600 MPa. There is also a report that the fatigue limit stress obtained from a rotation bending fatigue test is approximately 1000 MPa. We would like to mention that, in the present study, we determined the fatigue limit stress by applying the maximum defect distribution of regression values from extreme-value statistics, and came to the conclusion that a value of approximately 1600 MPa is appropriate. From the information regarding fracture of sintered alloy, there is no process of generation and propagation of cracks, and this is useful because the yield stress can be calculated by tracing back from the fracture toughness value if only the starting point is known. In the boundary of fractal dimension, by putting as K_{max} K_{IC}, $w_p=a+r_p$ from formula (2),

$$s_0=1.390s_y \tag{5}$$

The yield stress comes to about 70% of the repetitive stress. The crack propagation mechanism is different on the surface side from that with the internal starting point type. The fracture toughness value of the internal starting point type is approximately 60% of the value on the surface side. This is interpreted as resulting the difference in the state of plane strain and the state of plane stress.

Here is a summary of what has been described above.

(1) Height information by fractal dimension is an extremely important factor for knowing the form of fracture. If the distribution of 2-dimensional fracture at the same time is checked, it is useful because it enables us calculate the stress at any desired point P (x, y) at a distance r from the starting point.

(2) In the present study, we determined the dimension of plastic zone from Dugdale model, given by the following formula with crack propagation rate curve, i.e.

$$K_{max}=\frac{\Delta K}{(1-R)} \geqq K_{IC} \tag{6}$$

Formula (6) gives the condition of unstable fracture.

(3) The distribution chart in Fig. 5 indicates that breaking took place because of a crack produced in a very early period. Further progress into the shape of secondary curve can be understood from the fact that turning up was observed with the left and right test pieces because of a difference in the gradient of height.

(4) From Fig. 5, the fracture toughness value increases on the surface of the test piece. What is important is the point of separation and breaking, and the fracture toughness value at that point comes to approximately 9 $MPam^{1/2}$. This value agrees well with the value determined by CT test.

Figure 2 shows a micrographic photo observed at a magnification of 1500 of the test piece cut out in the axial direction after the test and etched with Murakami's reagent.

(5) Because one obtains $a = K_{max}/K_{IC} = 1.1215$:=const and the Hurst number takes a low value of 0.3 or so, the fluctuation of height can be presumed to be rather small.

References

[1] S.Palmqvist: Jernkontorets Ann., 141(1957), 300.
[2] J.L.Chermant and : J.Mater.Sci.,11(1976),1939.
[3] R.A.Almond, F. Osterstock B. Roebuck: Metals Tech., (1978), 92.
[4] Yukitaka Murakami, "Metal fatigue Effect of small defect and inclusion", Yokendo, 1992.